

# Revealing Interfaces and Nanostructure: The Application of Atom Probe Tomography to Nickel Based Superalloys

Dr. Chantal Sudbrack, NASA Glenn Research Center, [chantal.k.sudbrack@nasa.gov](mailto:chantal.k.sudbrack@nasa.gov)

1. Background in nickel-based superalloys
2. Background in atom-probe tomography
3. Decomposition behavior of model Ni-Al-Cr alloy when aged at 600 °C

*Acknowledgements: Prof. David Seidman, Kevin E. Yoon , Zungang Mao (Northwestern); Ronald Noebe (NASA GRC); Georges Martin (Comm. à l'Energie Atomique); Northwestern University Center for Atom Probe Tomography (NUCAPT)*

**Poster: The effect of prior exposures on the notched fatigue behavior of disk superalloy ME3**

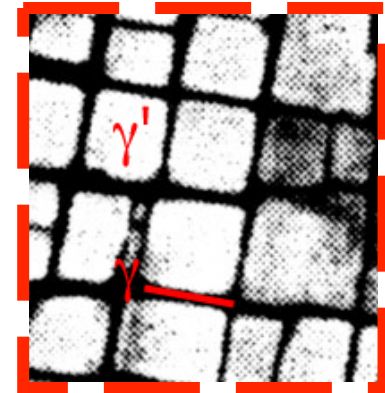
Co-authors: Susan L Draper<sup>1</sup>, Timothy T Gorman<sup>2</sup>, Jack Telesman<sup>1</sup>, Timothy P Gabb<sup>1</sup>, David R Hull<sup>1</sup>, Daniel E Perea<sup>3</sup> and Daniel K Schreiber<sup>3</sup> : 1. NASA Glenn 2. NASA USRP 3. PNNL



# Ni-Based Superalloys

Due to an unusual combination of properties, Ni-based superalloys are used in many applications which require structural integrity at elevated temperatures

Precipitate strengthened



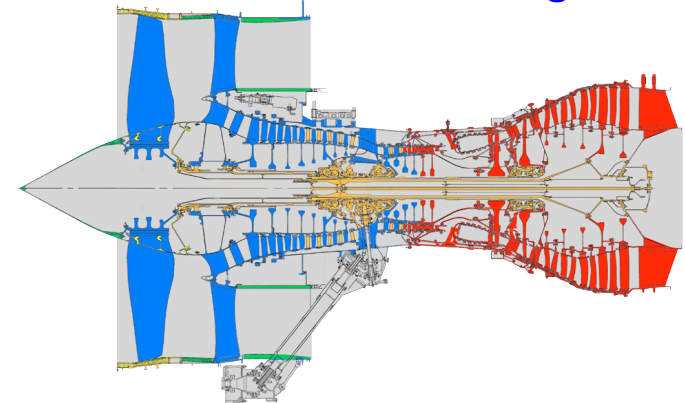
## Mechanical properties

- Capable of bearing loads at  $T/T_M = \sim 0.85-0.9$  ( $T_{M(Ni)} = 1453^\circ\text{C}$ ) without significant deformation
  - $\gamma'$  strengthening (precipitate strengthening)
  - Solid solution strengthening in the  $\gamma$ -matrix
- Damage Tolerance (Ductility and Toughness)

## Requirements:

- Resistance to Environmental Degradation
  - Hot corrosion and oxidation

Turbine Jet Engine

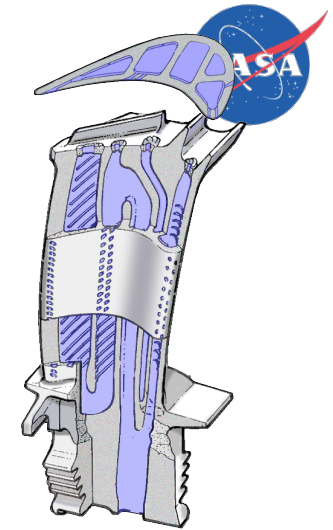


Titanium Steel Nickel

- **Single Crystal Ni-Based Superalloys**

- Engineered for Extreme Temperature Capability - Creep, Thermal Fatigue and Environmental Protection
- Anisotropic Properties
- Turbine Blade and Nozzle Applications

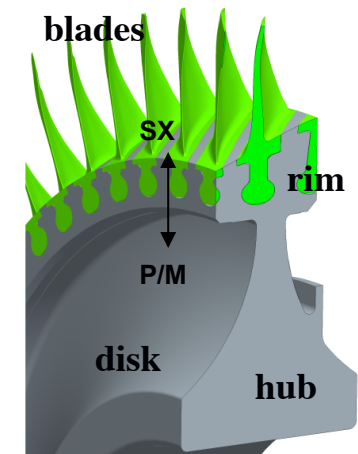
**NASA GRC**



- **Polycrystalline Ni-Based Superalloys**

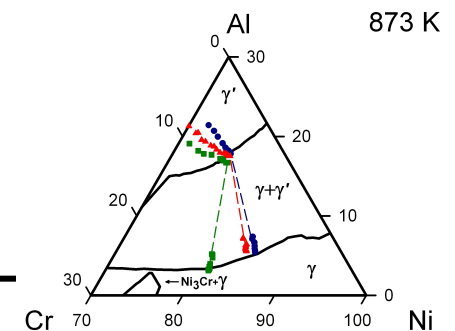
- Intermediate Temperature Capability – Fatigue, Tensile, Crack Growth and Environmental Resistance
- Isotropic Properties
- Turbine Disk Applications

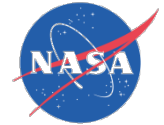
**NASA GRC**



- **Model Ni-Based Superalloys**

- Fundamental thermodynamic and kinetic underpinning of  $\gamma'$ -precipitation



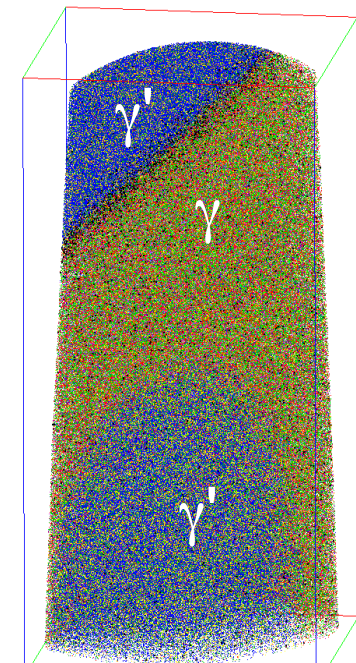


# Atom-probe tomography measurements

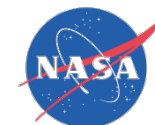
**APT:** post-mortem atomic imaging technique in direct space with sub-nanometer spatial resolution (static snapshots of dynamic process)

1. Short-range ordering, clustering, impurity concentration & distribution
2. Morphological development
3. Dimensional and nanostructural quantification
  - Variations in layer thicknesses
  - Radius, number density, volume fraction of precipitates
4. Compositional characterization
  - Bulk phases
  - Fine scale nanostructure
  - Buried interfaces (e.g. grain boundaries):
    - Chemical interdiffusion, chemical roughness, segregation, transients

~50 million atoms



98 nm x 97 nm x 152 nm



# 3-D Atom Probe Tomography

Local Electrode Atom Probe (LEAP™) Imago Scientific 3000XSi

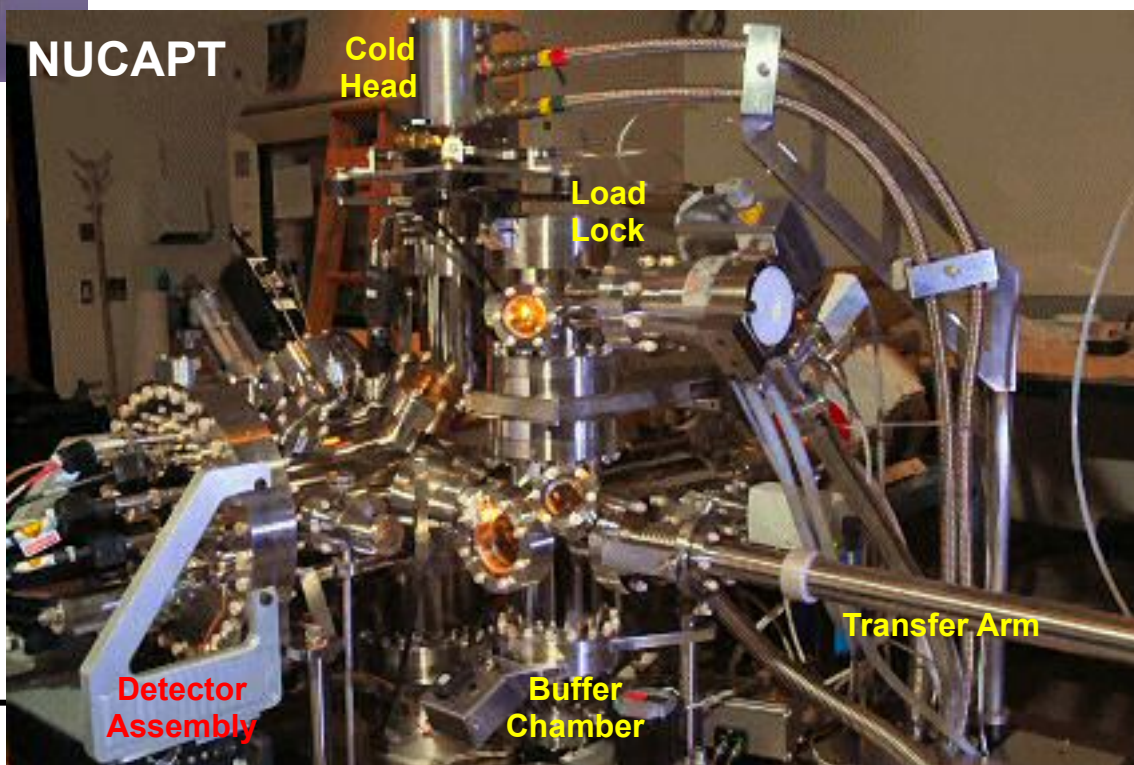


- Analyze data with 3D visualization software, IVAS, from Cameca (formerly Imago Scientific)

Determines the spatial position of individual atoms and their chemical identities with sub-nanometer scale resolution

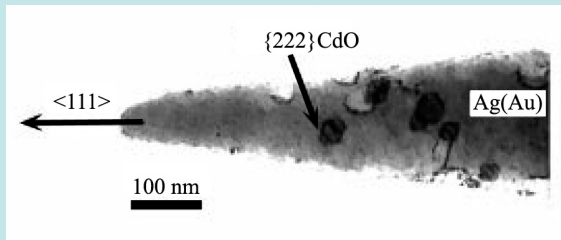
Ion detection efficiency: 40-60%, Depth positioning: 0.02-0.05 nm, Lateral positioning: 0.2-0.3 nm

- Analyze volumes  $>10^6 \text{ nm}^3$   
 $0.1 \times 0.1 \times 0.5 \mu\text{m}^3$
- $5 \times 10^{-11}$  torr ultrahigh vacuum
- Specimen T: 20 to 300 K
- Equipped with both electrical and thermal-assisted pulsing:
  - 250 kHz electrical pulse
  - 500 kHz picosecond laser  
(green: 532 nm, 10 ps)



# APT specimens are needle shaped

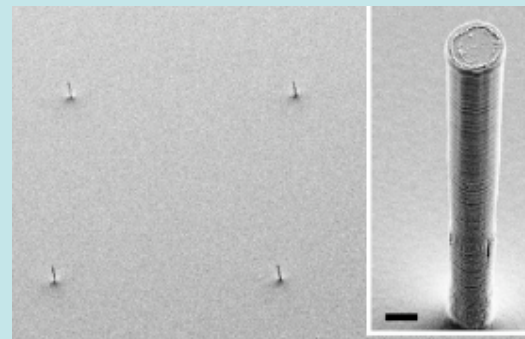
**Metals:** Electrochemical wire sharpening from APT blank (0.25 x 0.25 x 10 mm<sup>3</sup>)



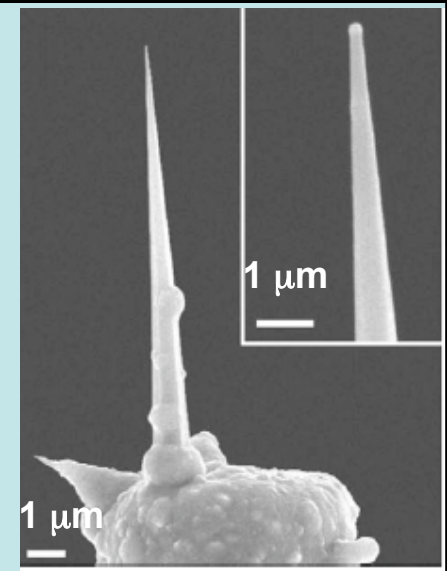
D. A. Shashkov, M. F. Chrisholm and D. N. Seidman  
*Acta. Mater.*, 47, 3939-3951 (1999).

**Nanowires:** Direct growth on a micropost

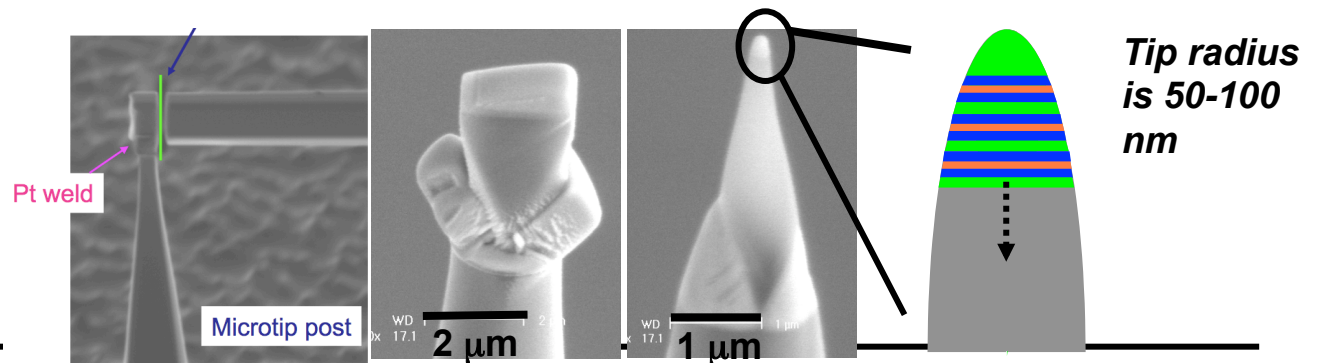
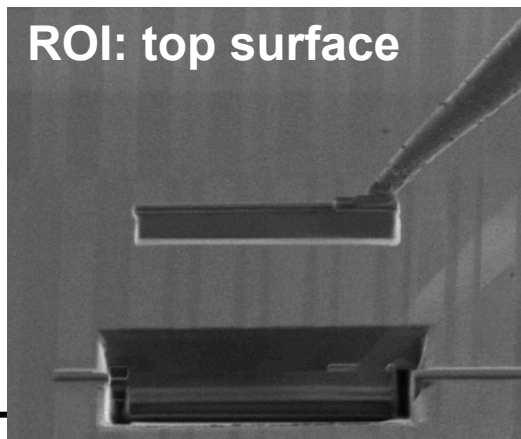
Silicon Micropost Array



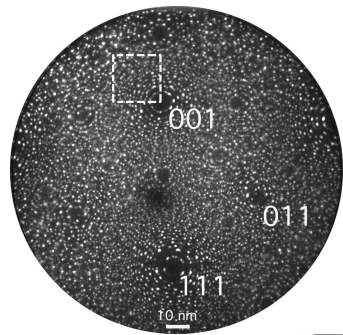
*Perea et al. J. Solid State Chem*, 181 (2008) 1642



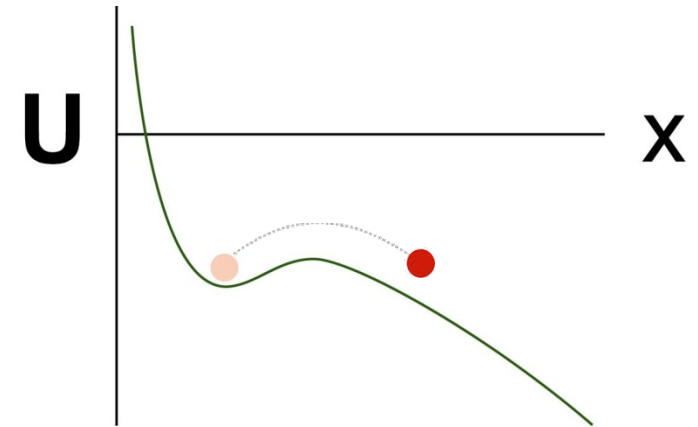
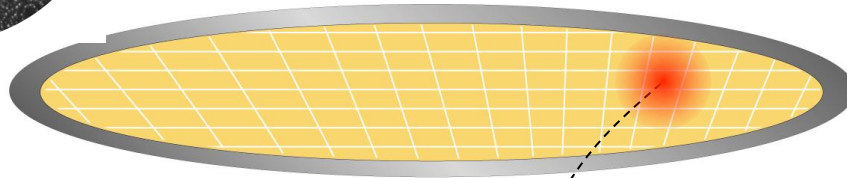
**Multilayers:** FIB preparation / Lift-out to micropost



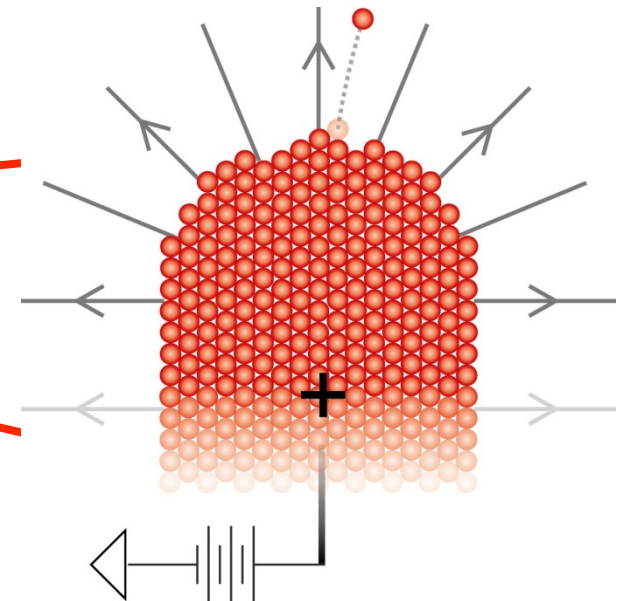
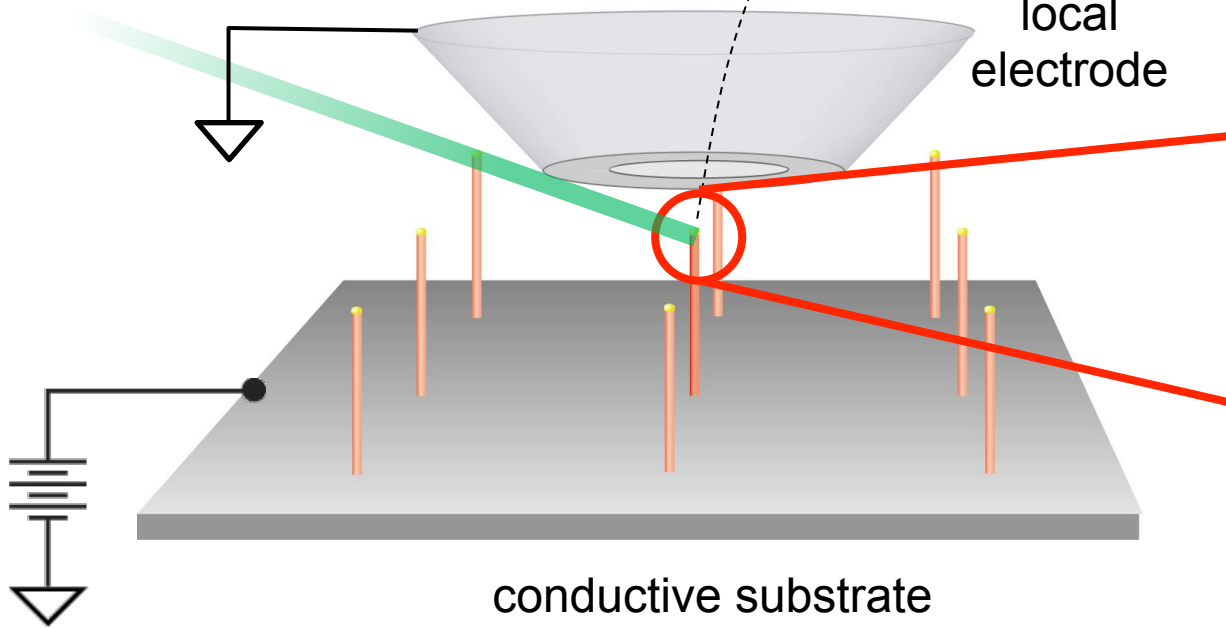
# Pulsed-laser Atom Probe Tomography



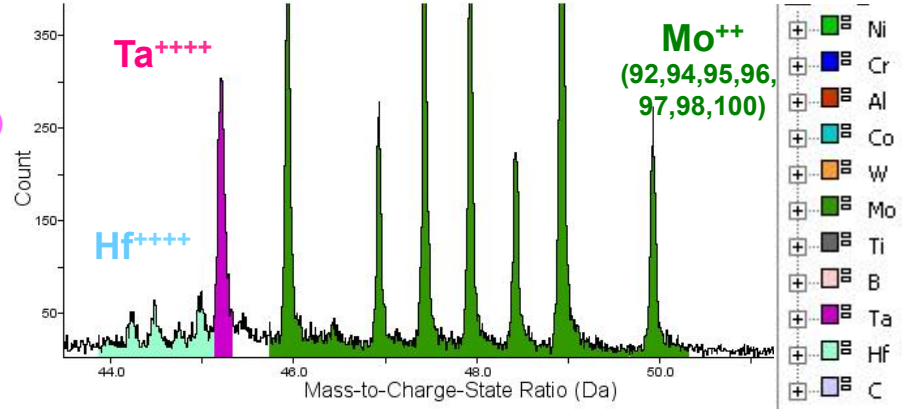
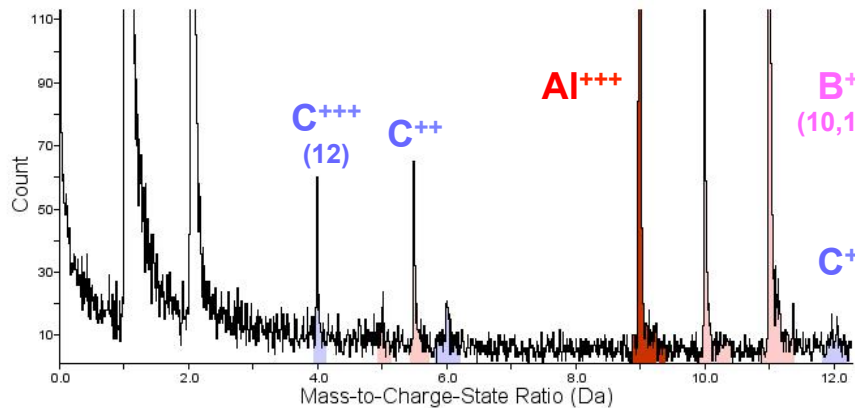
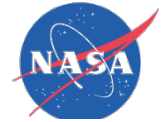
position-sensitive TOF detector



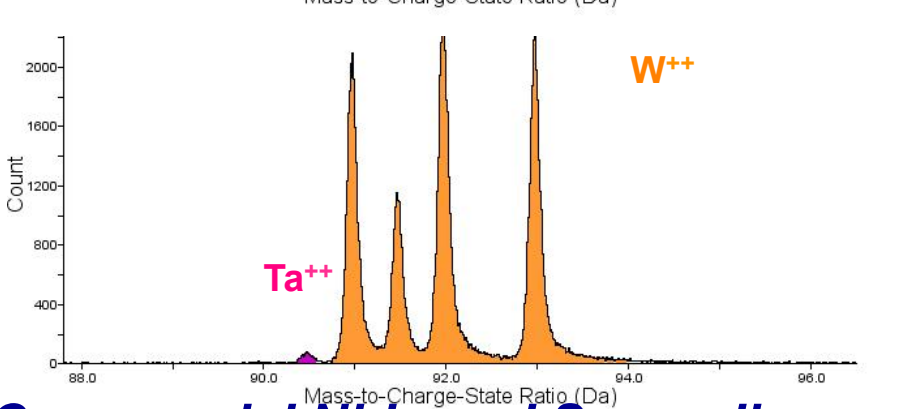
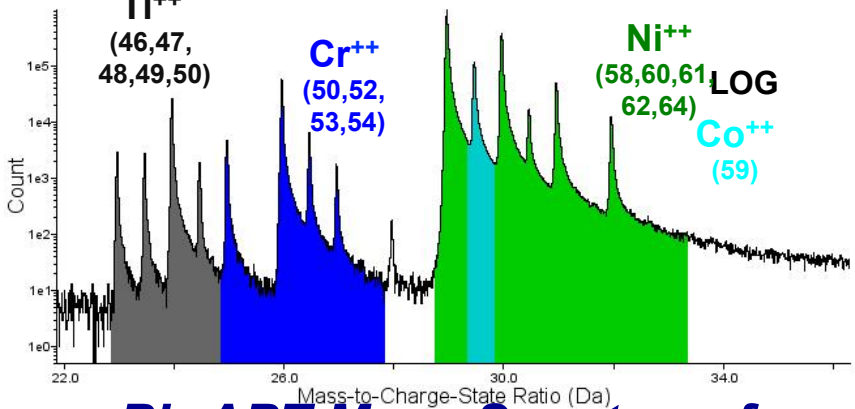
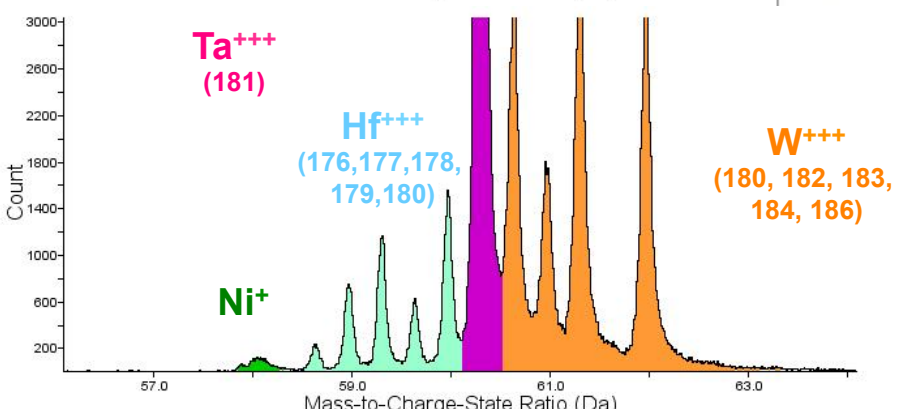
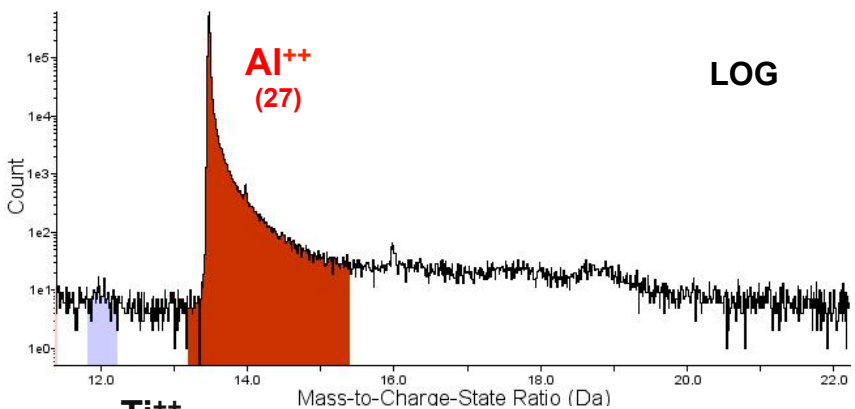
local electrode



# Ions identified from their m/n signature (time-of-flight)

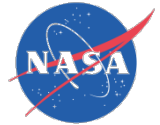


<input checked="" type="checkbox"/>	Ni
<input checked="" type="checkbox"/>	Cr
<input checked="" type="checkbox"/>	Al
<input checked="" type="checkbox"/>	Co
<input checked="" type="checkbox"/>	W
<input checked="" type="checkbox"/>	Mo
<input checked="" type="checkbox"/>	Ti
<input checked="" type="checkbox"/>	B
<input checked="" type="checkbox"/>	Ta
<input checked="" type="checkbox"/>	Hf
<input checked="" type="checkbox"/>	C



**PL-APT Mass Spectrum for a Commercial Ni-based Superalloy**





# 3-D LEAP™ Tomography

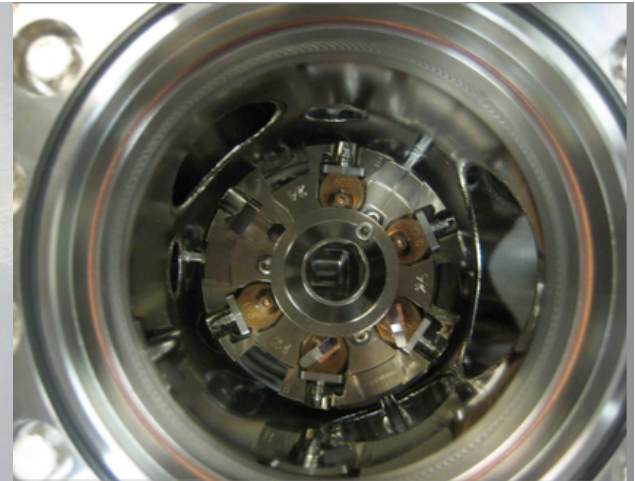
**Specimens & Pucks**



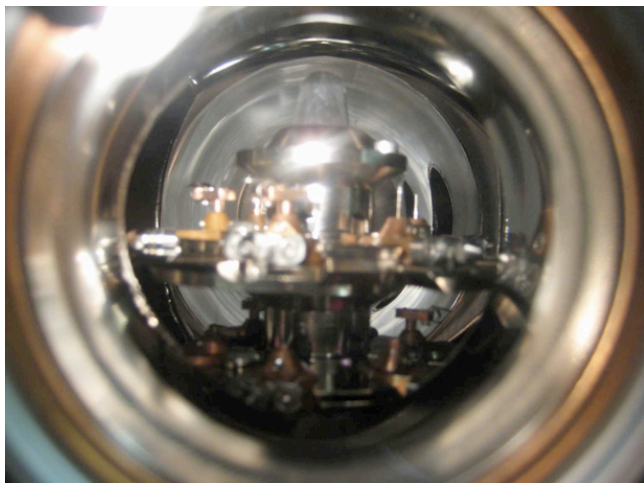
**Specimen Carousel**



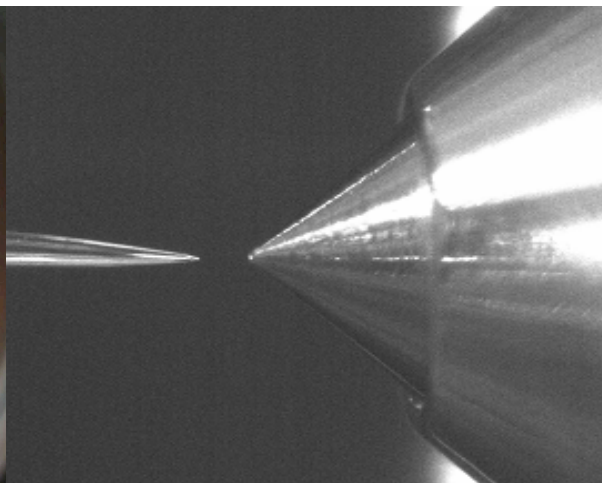
**Load Lock Chamber (Top Entry)**



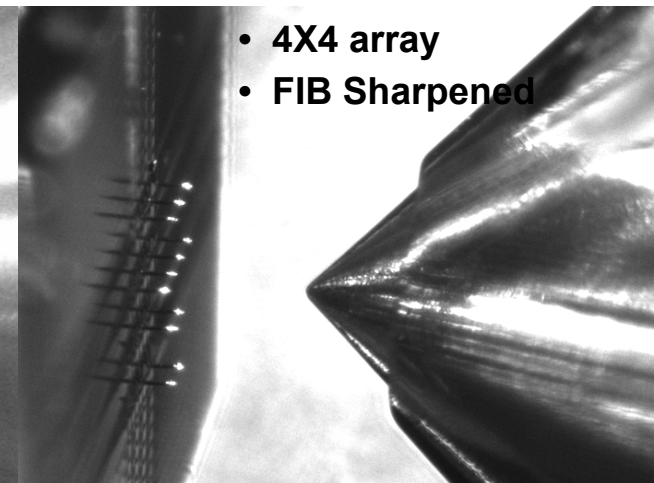
**Analysis Chamber (Side Viewport)**



**Needle Geometry**

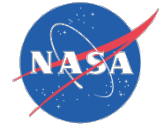


**Microtip Geometry**



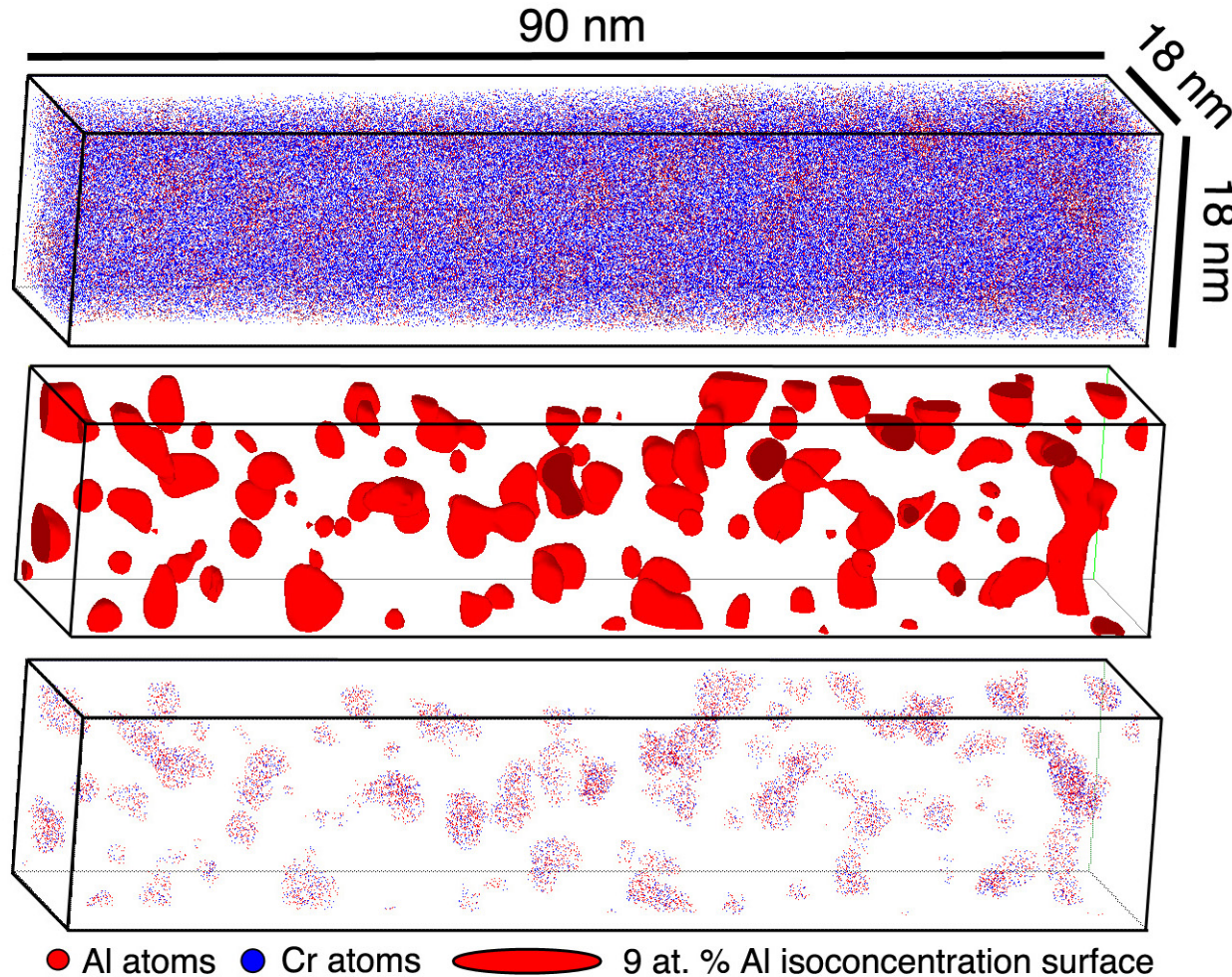
Courtesy of NUCAPT

Courtesy of Imago



# Fine scale microstructural analysis with APT

Ni-5.2 Al-14.2 Cr (at. %) aged at 600°C for 4 hours



**APT  
reconstructed  
volume**

**Isoconcentration  
surface**

**Selected  
volume**

# Proximity Histogram Concentration Profile

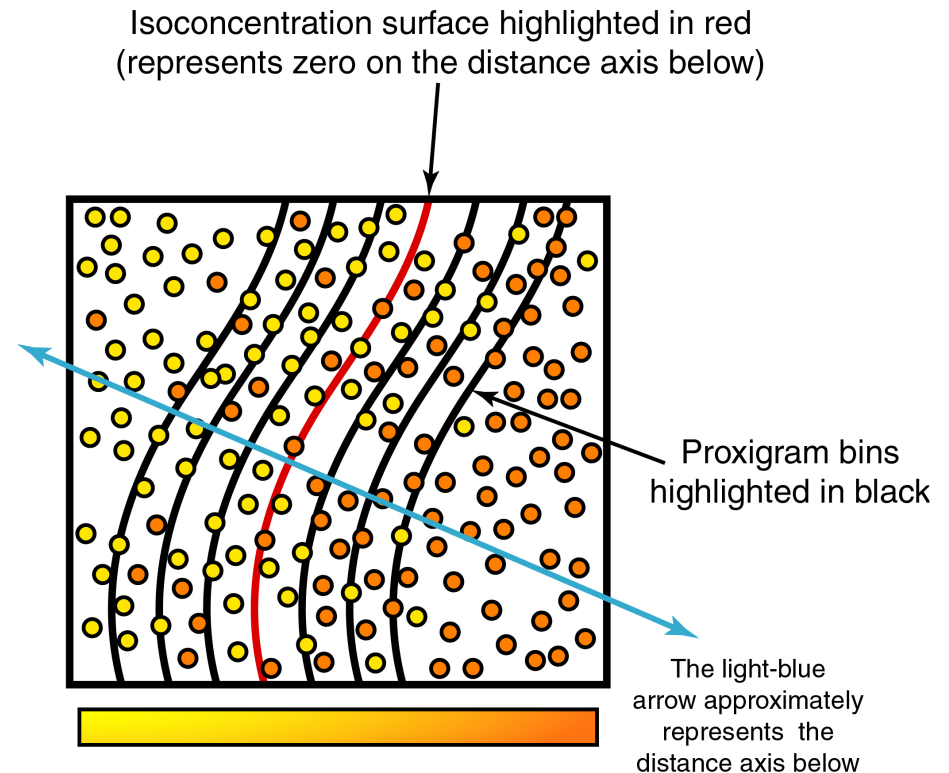
## Data analysis in IVAS 3D visualization software



Proximity Histogram or “Proxigram” is a 3D nonlinear compositional profile with respect to isoconcentration surface (interfaces).

### Three steps

1. A sampling to generate a regular grid of concentration points
2. An interpolation to identify an isoconcentration surface
3. A correlation of the isoconcentration surface to the original set of discrete atomic positions

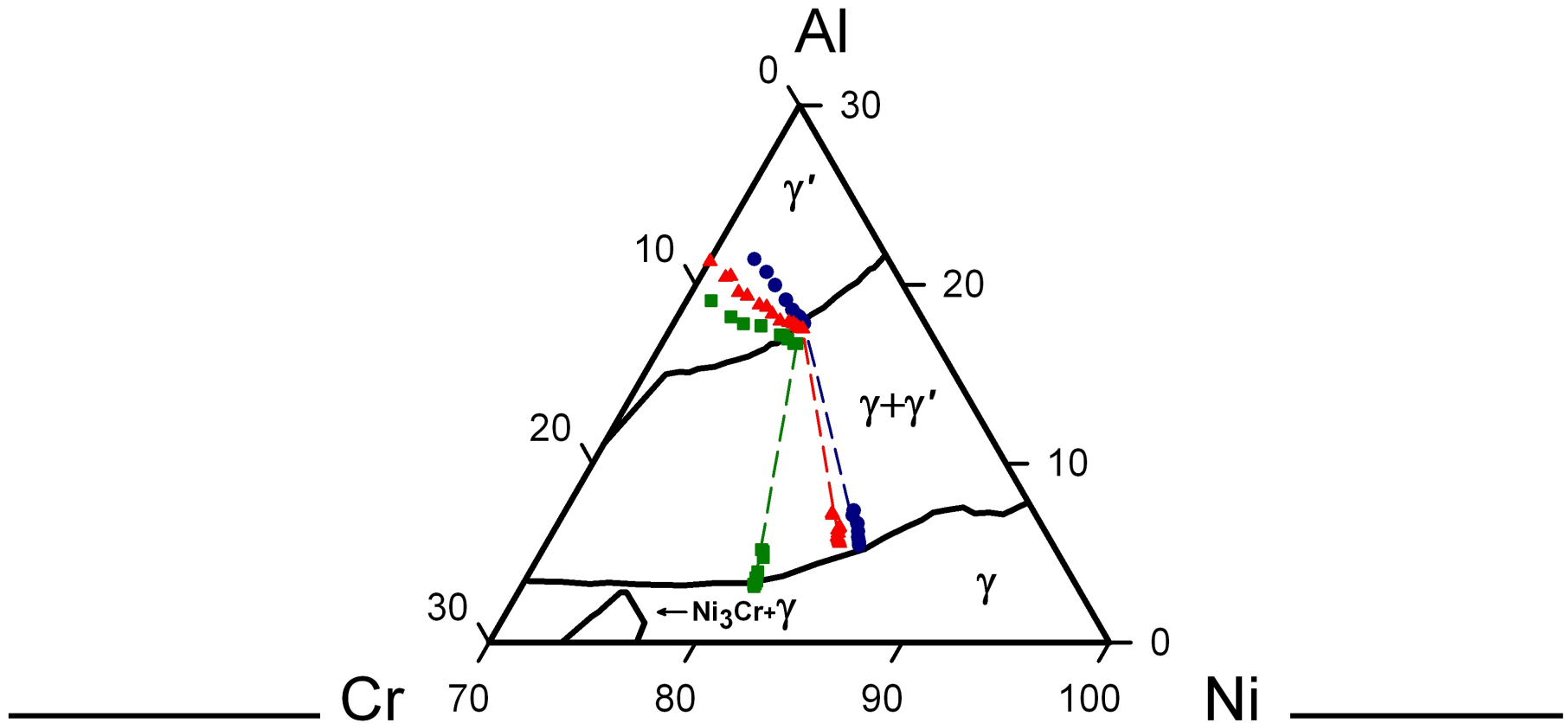


- Analyzes all the concentrations of the same value in a data set in parallel, invaluable for large data sets
- Invariant to interfacial geometry

Hellman, Seidman et al. *Micro. Microanal.* **6**, 437 (2000)



# Decomposition behavior of model Ni-Al-Cr alloy when aged at 600 °C

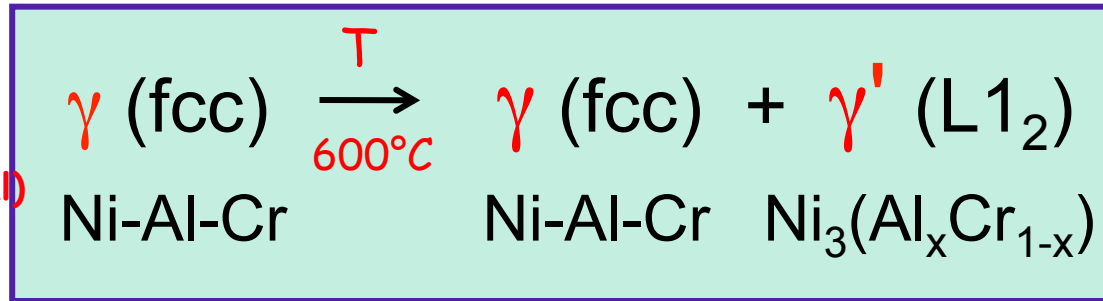




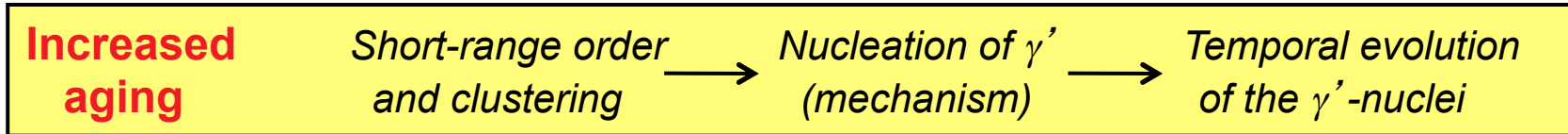
# T= 600 °C aging studies of Ni-5.2 Al-14.2 Cr at. %

## Atomic-scale mechanisms that drive the early stage precipitation

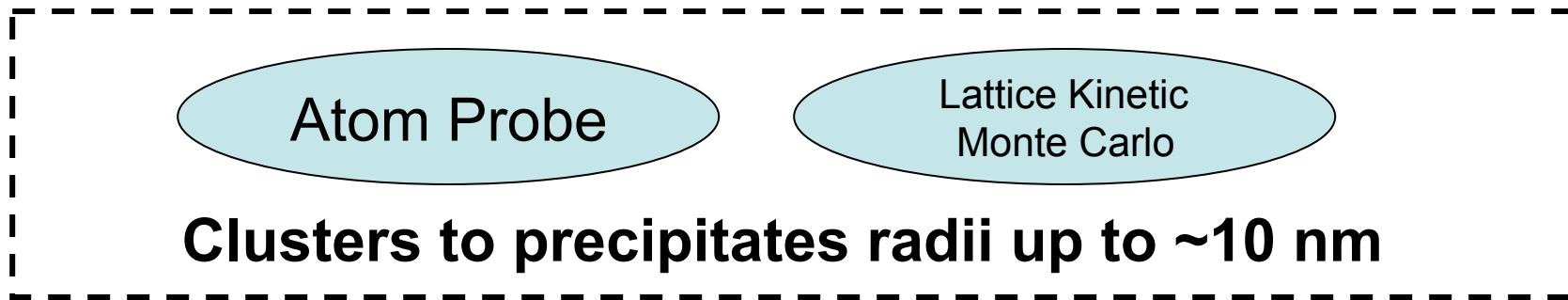
Moderate solute  
supersaturations,  
 $\phi^{eq} = 15.6\%$   
(nondilute, nonideal)



1<sup>st</sup>-order  
ordering  
transformation



### Nanostructural & Compositional Evolution



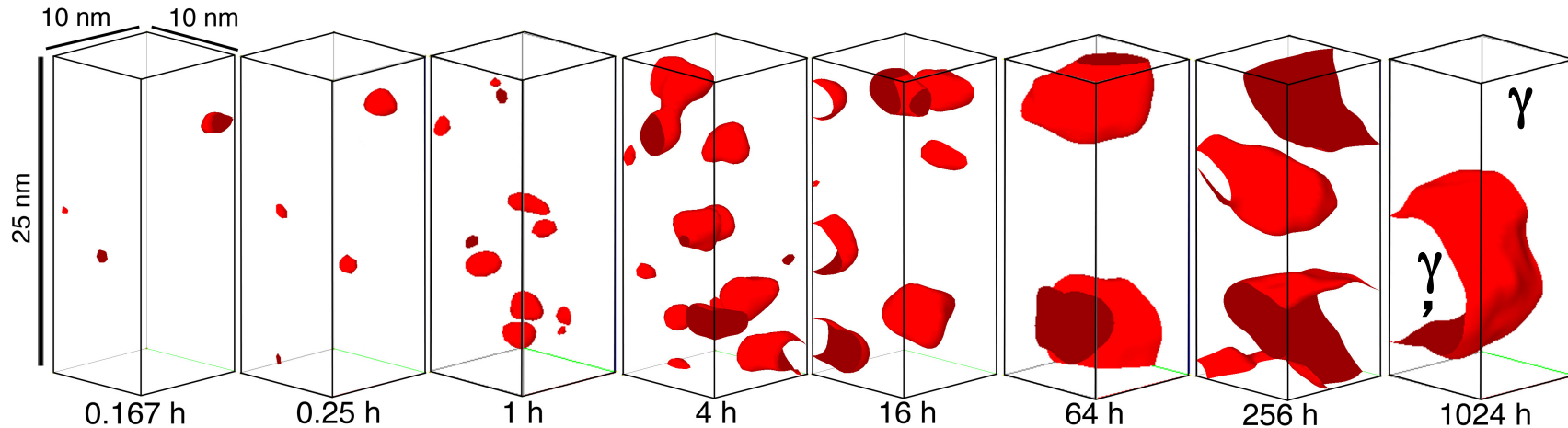
Seminal research of Schmuck *et al.* (Phil. Mag. A **76**, 1997, p.527)  
and Pareige *et al.* (Acta mat. **47**, 1999, p.1889)

# Temporal evolution of $\gamma'$ -precipitation in 3D



10 x 10 x 25 nm<sup>3</sup> sub-volumes of APT reconstructions

9 at. % Al isoconcentration surfaces (atoms omitted for clarity)



*Ni-5.2 Al-14.2 Cr aged at 600°C*

- **Precipitates as small as  $R = 0.45$  nm are resolved, 20 detected atoms, which is close to lattice kinetic Monte Carlo (LKMC) predictions for critical nuclei size of 0.485 nm**
- **Dimensions and orientation of each precipitate are determined using best-fit ellipsoid**
- **Buried interfaces: generate average compositional profiles across the  $\gamma/\gamma'$  interfaces using proximity histogram compositional profiles**



# APT measurements of the mean precipitate radius

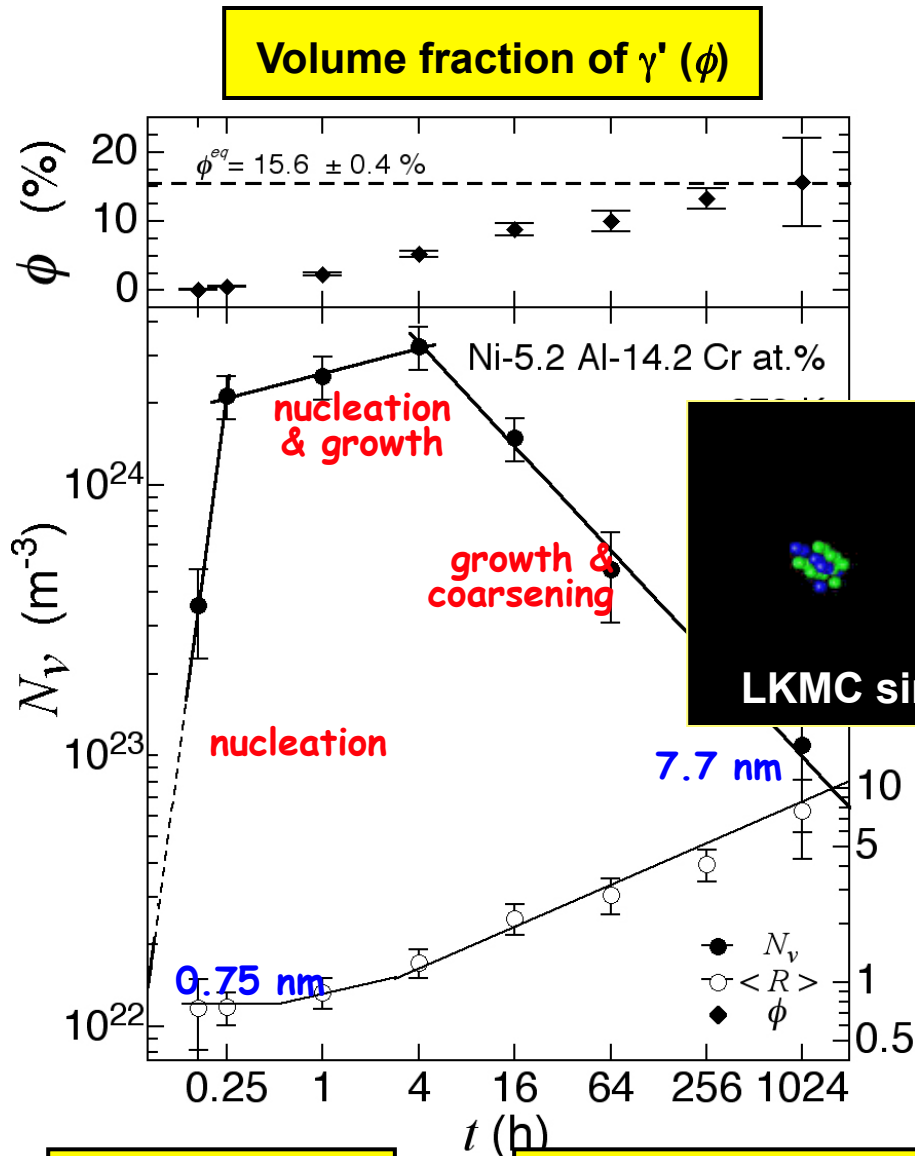
$t$ (h)	Nb. of ppts. analyzed	$\langle R \rangle \pm \sigma$ (nm)
0.17	7.5	$0.74 \pm 0.24$
0.25	74	$0.75 \pm 0.14$
1	100	$0.89 \pm 0.14$
4	173.5	$1.27 \pm 0.21$
16	101	$2.1 \pm 0.4$
64	46	$2.8 \pm 0.6$
256	81	$4.1 \pm 0.8$
1024	6	$7.7 \pm 3.3$

nucleation

nucleation  
and growth

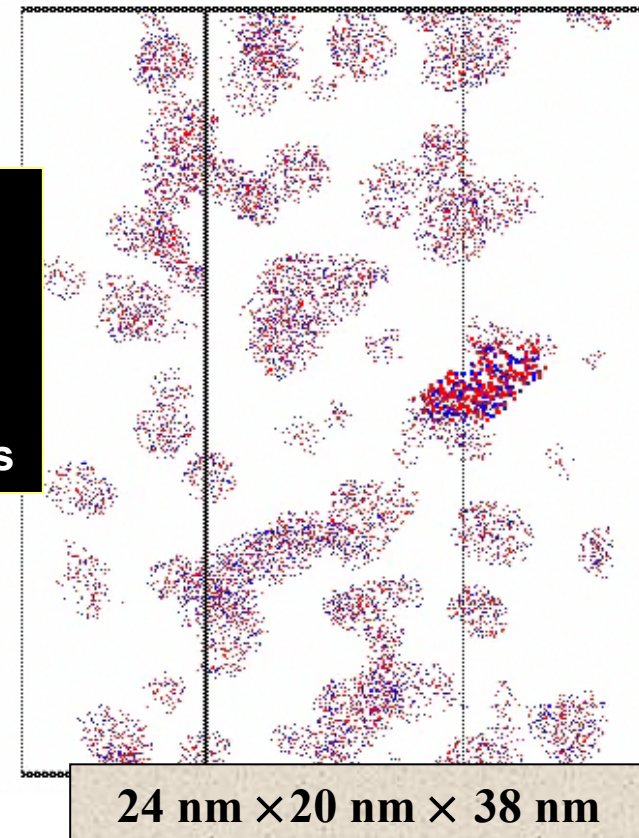
growth and  
coarsening

# Growth regimes established by APT measurements



Example of  $\gamma'$ -precipitate pair connected by necked region

$t = 4 \text{ h}$  at peak  $N_v$



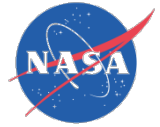
**Ppts. per unit volume ( $N_v$ )**

**Mean precipitate radius ( $\langle R \rangle$ )**

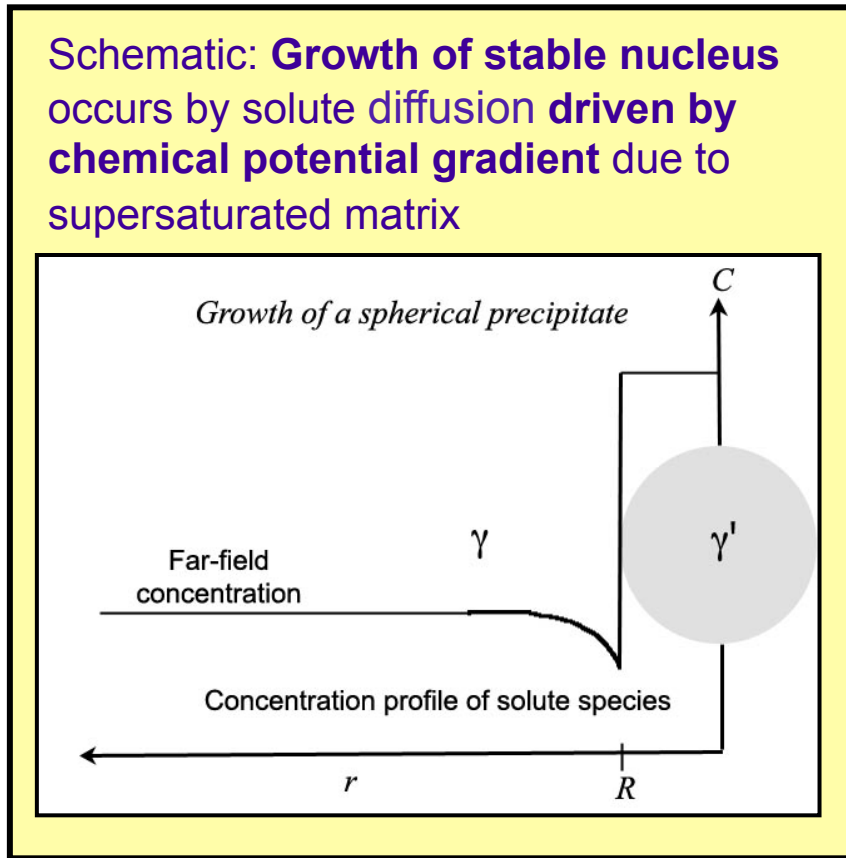
**Al and Cr atoms within the 9 at. % Al isoconcentration surface displayed**

Sudbrack et al, Acta Mater 54 (2006) 3199. [www.nasa.gov](http://www.nasa.gov)



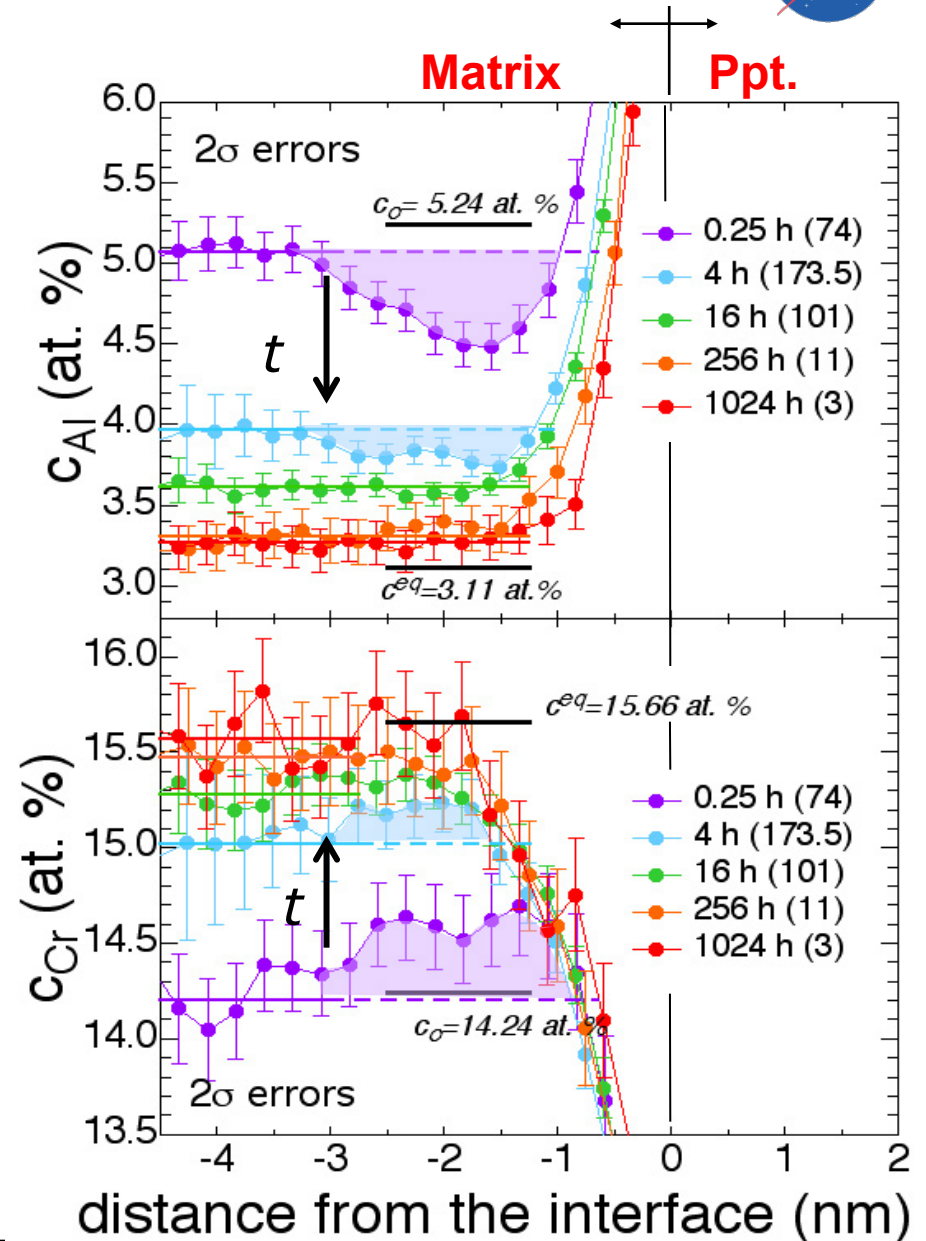


# Concentration profile evolution in the matrix



➔ *Transients disappear after 16 h  
∴ quasi-steady state obtained*

*F. S. Ham, J. Phys. Chem. Solids, 6 (1958) 335*

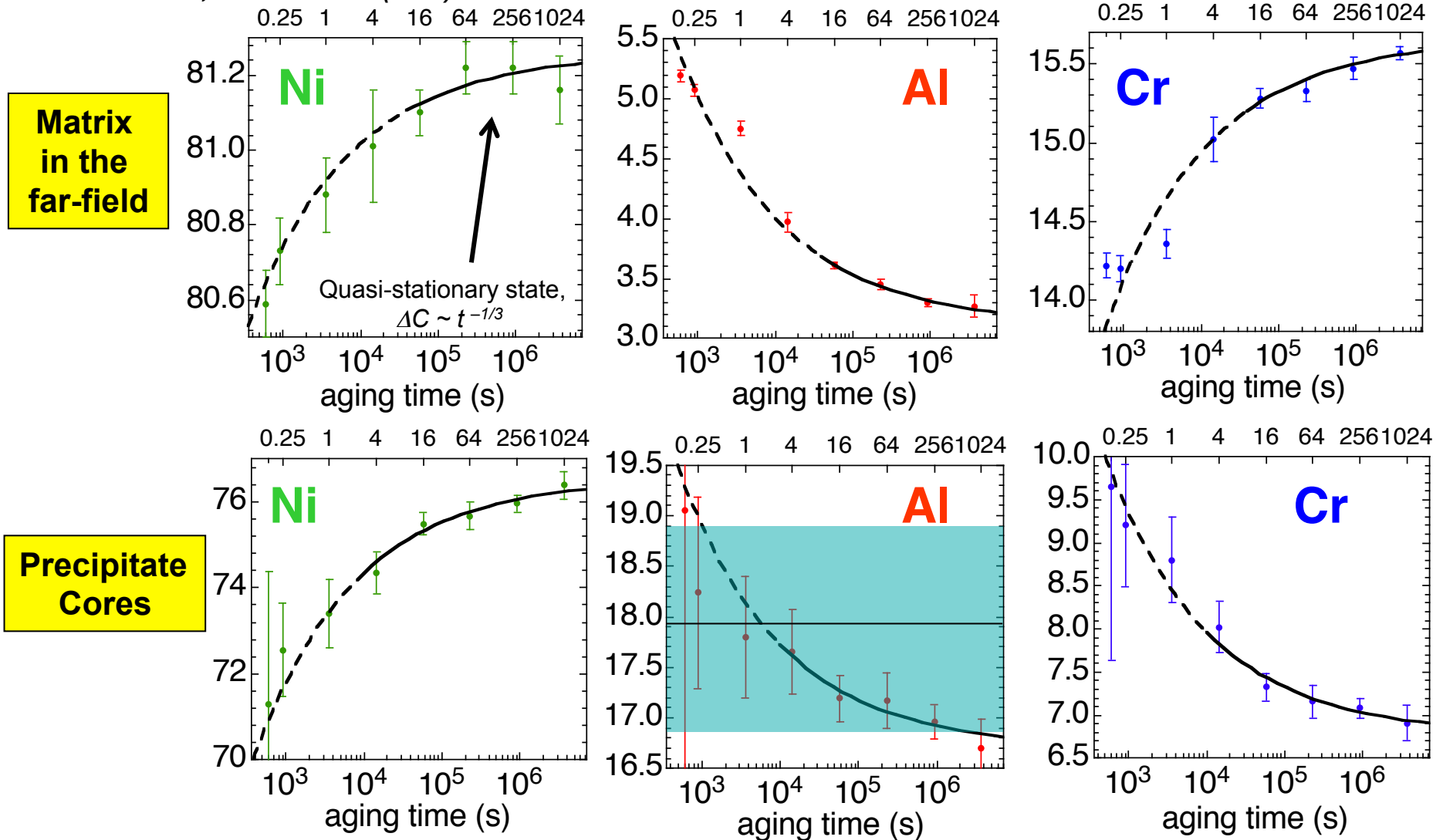


\* **Proxigram method, which averages over all interfaces in the analysis volume** www.nasa.gov 16

# Compositional evolution



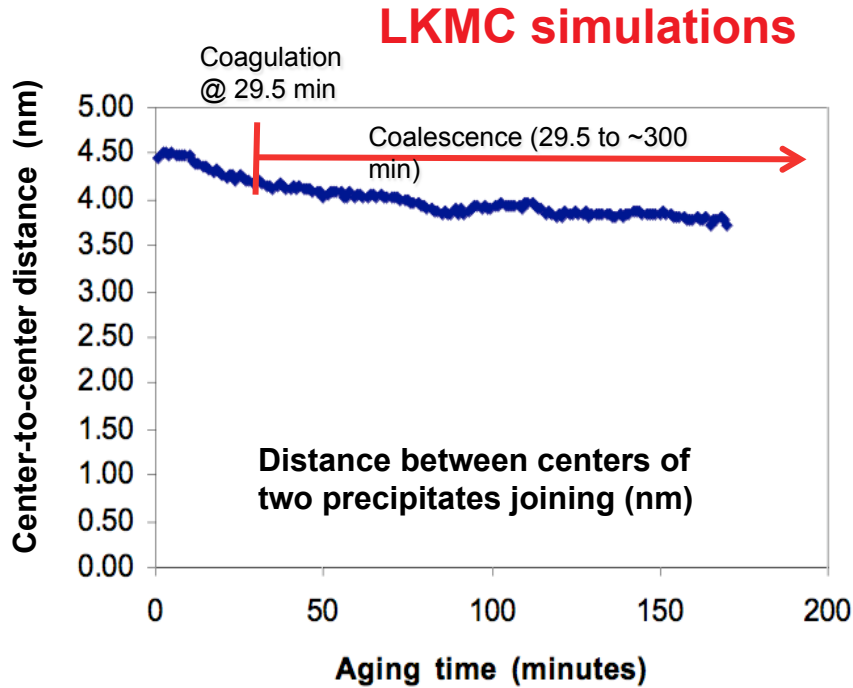
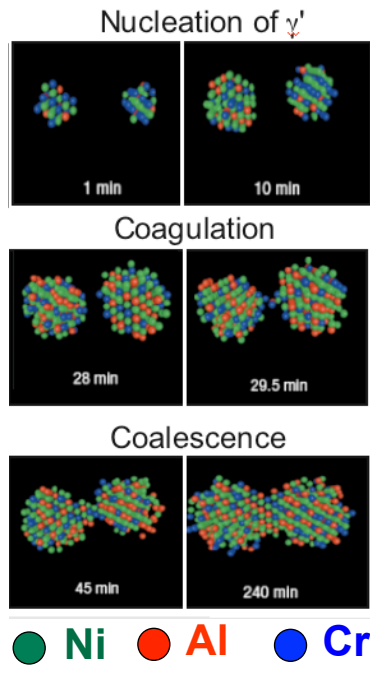
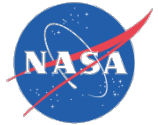
Sudbrack et al, *Acta Mater* 54 (2006) 3199.



**Gibbs-Thomson effect:** predicts an increase in solid-solubility at an interface due its curvature. It is non-negligible when precipitate dimensions are on the of the order capillary length, typically 1-2 nm

See: *Sudbrack et al, Acta Mater* 55 (2007) 119.

# Confirmation of early-stage coagulation & coalescence



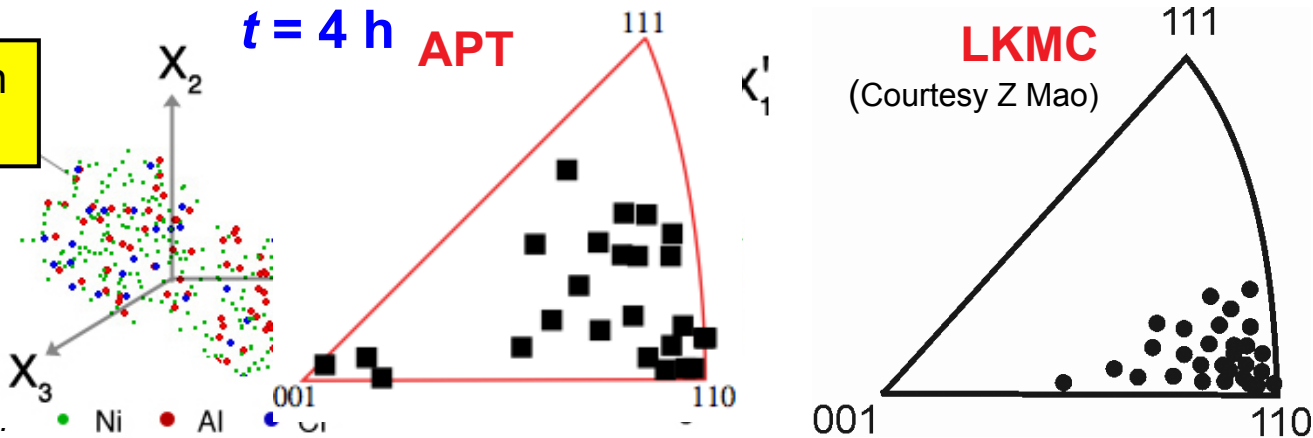
There are four  $L1_2$  ordering variants

APB energy for two variants to join is 3-4 times larger than interfacial energy

--> Two precipitates must match variants to join

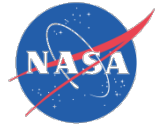
As much as 30% coalesced

Neck orientation distribution



RA Karnesky, CK Sudbrack and DN Seidman, APL (2007).

In FCC structure of the  $\gamma$ -matrix,  $\langle 110 \rangle$  is fastest diffusion path for solute clusters



- **Atom probe tomography is a powerful characterization technique**
- **The combined APT/LKMC approach has been particularly helpful in:**
  - Nanometer scale characterization of morphological development in 3D
  - Precise compositional analysis of buried interfaces
  - Insight into diffusional processes that drive phase transformations